

Nanoscale

Accepted Manuscript



This is an *Accepted Manuscript*, which has been through the Royal Society of Chemistry peer review process and has been accepted for publication.

Accepted Manuscripts are published online shortly after acceptance, before technical editing, formatting and proof reading. Using this free service, authors can make their results available to the community, in citable form, before we publish the edited article. We will replace this *Accepted Manuscript* with the edited and formatted *Advance Article* as soon as it is available.

You can find more information about *Accepted Manuscripts* in the [Information for Authors](#).

Please note that technical editing may introduce minor changes to the text and/or graphics, which may alter content. The journal's standard [Terms & Conditions](#) and the [Ethical guidelines](#) still apply. In no event shall the Royal Society of Chemistry be held responsible for any errors or omissions in this *Accepted Manuscript* or any consequences arising from the use of any information it contains.

Unraveling the complexity of the interactions of DNA nucleotides with gold by single molecule force spectroscopy

Fouzia Bano[†], Damien Sluysmans, Arnaud Wislez, Anne-Sophie Duwez^{*}

University of Liège, Department of Chemistry, B6a Sart-Tilman, 4000 Liège, Belgium

KEYWORDS: DNA, Gold, AFM Force Spectroscopy, nanotechnology, single molecule

ABSTRACT: Addressing the effect of different environmental factors on the adsorption of DNA to solid supports is critical for the development of robust miniaturized devices for applications ranging from biosensors to next generation molecular technology. Most of the time, thiol-based chemistry is used to anchor DNA on gold -a substrate commonly used in nanotechnology- and little is known about the direct interaction between DNA and gold. So far there have been no systematic studies on the direct adsorption behavior of the deoxyribonucleotides (i.e, a nitrogenous base, a deoxyribose sugar, and a phosphate group) and on the factors that govern the DNA-gold bond strength. Here, using single molecule force spectroscopy, we investigated the interaction of the four individual nucleotides, adenine, guanine, cytosine, and thymine, with gold. Experiments were performed in three salinity conditions and two surface dwell time to reveal the factors that influence nucleotide-Au bond strength. Force data show that, at physiological ionic strength, adenine-Au interactions are stronger, asymmetrical and independent of surface dwell time as compared to cytosine-Au and guanine-Au interactions. We suggest that in these conditions only adenine is able to chemisorb on gold. A decrease of the ionic strength significantly increases the bond strength for all nucleotides. We show that moderate ionic strength along with longer surface dwell period suggest weak chemisorption also for cytosine and guanine.

INTRODUCTION

Throughout the past decade, there has been increasing efforts towards extreme miniaturization of devices and smart sensors, which are expected to detect and quantify the presence of a substance but also to handle *in situ*, in a simple way, the information obtained¹⁻³. Deoxyribonucleic acid (DNA) functionalized gold surfaces, both planar and nanoparticles, have attracted huge attention of researchers in many disciplines of nanotechnology and biotechnology. For example, the immobilization of modified or thiolated DNA molecules on gold, obtained by self-assembly processes and other methods, have been intensively investigated for developing DNA-based assays such as DNA micro- or nano- arrays⁴⁻⁷. Despite their important role in the surface functionalization process, rather little is known about the direct interaction between DNA and gold.

Previous studies concerned the interactions of DNA bases (i.e, without sugar and phosphate groups) and were carried out by ensemble measurements. For example, Mirkin and coworkers reported on nonspecific interactions between nucleobases and gold with temperature programmed desorption (TPD), and reflection absorption FT infrared (RAIR) spectroscopy. These studies evidenced the sequence dependence in the binding behaviors of these small units of DNA⁸. Similar trends have been observed for DNA adsorption on nanoparticles by Li and Rothberg. In their study, the effect of sequence length and temperature on the rate of DNA adsorption to gold nanoparticles has been reported and rationalized on the basis of electrostatic interactions⁹. Those ensemble experiments have shown that both adhesive and cohesive interactions contribute the apparent binding energies to the substrate surface. We can thus hardly conclude on the binding strength of the species. Furthermore, the studies suggest that the presence of the sugar and phosphate groups could decrease the binding strength of the DNA bases. They likely sterically inhibit the bases from adopting their most strongly bound orientation, resulting in various degrees of destabilization. So far, a quantification of the interactions between the nucleotides and gold at the single nucleotide level is still lacking. To the best of our knowledge, there is only one study on the adsorption behavior of single nucleotides on gold. The strength of the adenine-gold bond as a function of surface potential has been measured and suggested for a potential immobilization approach¹⁰. The absence of a systematic study for all nucleotides is mainly due to the complex correlation between DNA properties (composition, charge, shape and flexibility), surface properties (morphology, surface charge density and hydrophobicity) and solution composition (pH, ion charge density and valence number)¹¹.

Atomic force microscopy (AFM)-based single molecule force spectroscopy (SMFS) has previously been largely applied for understanding the framework of interactions in biological processes as well as the adsorption of molecules on surfaces¹²⁻¹⁴. Here, we have used SMFS to systematically investigate the interactions between all deoxyribonucleotides (i.e, a nitrogenous base, a deoxyribose sugar and a phosphate group) and gold. The measurements are done in liquid, at the single molecule level. There is thus no contribution from cohesion, unlike the previous studies reported so far^{8, 9}. Specifically, we have studied the effect of ionic strength and surface dwell time on the nucleotides-gold interactions.

RESULTS AND DISCUSSION

To probe the interactions between the different nucleotides and gold, the AFM tip was functionalized with two different DNA oligomer systems. The first one is a homo-oligomer of 20 nucleotides: SH-(CH₂)₆-5'-X₂₀-3' (X₂₀, where X= T, C, G, or A). The other one is made of a 24 thymine spacer and 2 specific nucleotides: SH-(CH₂)₆-5'- T₂₄X₂-3', (T₂₄X₂, where X = A, C, or G). The choice of the poly(thymine) spacer was dictated by the fact that it is known to behave as a linear polymer with no stacking interactions between the bases¹⁵. The length of the DNA oligomers is chosen to be long enough to avoid any non-specific interactions between the AFM tip and surface. The thiol group is used to anchor the DNA single strand on the gold-coated tip. The tip was then gently approached to the gold substrate (Figure 1a. See the Experimental Section for details). After a contact time allowing the DNA bases to interact with Au, the tip was withdrawn at a constant pulling rate.

X₂₀ – Au interactions

Normalized force-extension curves (Figure 1b) show that thymine (T) has very weak interaction with gold as compared to all other nucleobases (A, C and G) under physiological ionic strength. Histograms of forces for these four nucleotides are shown in Figure 1c, where peak position is related to the most probable nucleotide-Au bond strength, while the width of the histogram can reveal variations in the binding geometry (adsorption) with the surface (besides the statistical error). Only on the force histogram for nucleotide A (Figure 1c, top left), we found two peaks, positioned at $78 \pm 5\text{pN}$, and $180 \pm 10\text{pN}$ (see the ESI for details on the data analysis). The origin of this multiple peak histogram will be discussed later in details. This could indicate that adenine can bind through different types of interactions with gold¹⁰ or that multiple adenine units

can interact with gold at the same time. The fact that we do not observe multiple peaks for the other nucleotides is in favor of the first explanation. Moreover, histograms of rupture lengths i.e., distances of rupture force from contact point (Figure S1, Table 1) for all DNA sequences show a unimodal distribution, confirming that we are measuring the interactions between the extremity of X_{20} and gold. Note that the rupture force value observed for the second peak, 180 pN, is in the same range as the value observed by Gaub and co-workers (170 pN) for the electrically-induced chemisorption of adenine to gold¹⁰. This issue will be discussed in the next section. It has previously been shown that on gold, the strength of interactions likely depends on the ability of the bases to bind to the substrate due to the different types of possible surface binding elements (e.g. amides and carbonyls; mono- versus polydentate)⁸. In addition, it has been recently shown that the binding of molecules composing of adenine is highly favorable on gold^{10, 11, 16}.

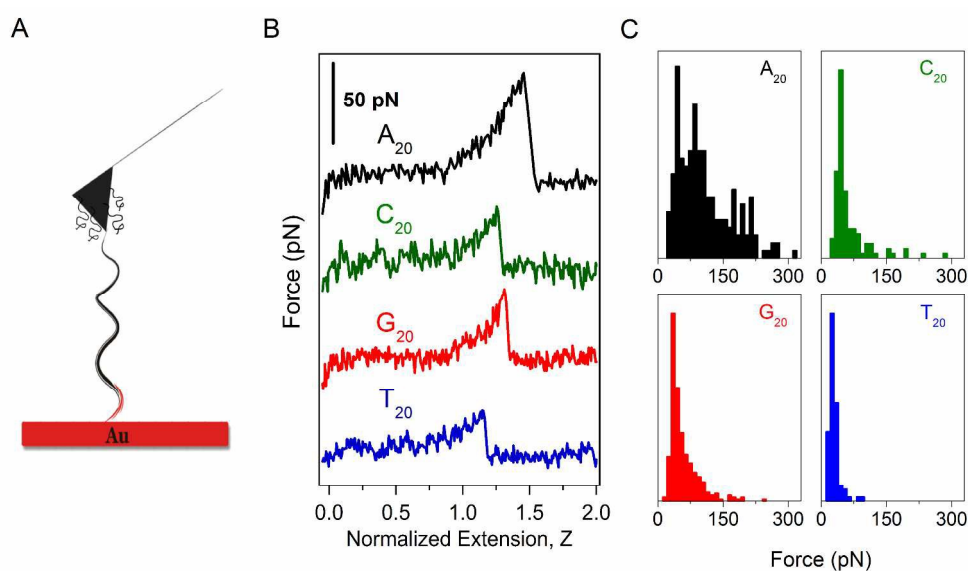


Figure 1: (A) Schematic representation of the SMFS experiments to measure the interaction between the nucleotides and gold (not to scale) (B) Normalized force-extension curves of four different DNA strands showing the rupture of the bond formed between the nucleobases and Au in 150mM NH_4OAc . All curves are normalized to $Z=1$ at $F=20$ pN which is the highest force value found in the case of T_{20} close to rupture point. (C) Histograms of rupture forces for A_{20} (black), C_{20} (green), G_{20} (red), and T_{20} (blue).

We estimated the desorption energies of each nucleotide by using the rupture force values and bond length of 0.5 nm, and compared with the binding energy estimated in DFT calculations performed with the PW91 exchange-correlation function for nucleobases on Au (Table 1)¹⁷. The values are consistent. The exception is adenine with average desorption energy of 23.6 ± 0.02 kJ mol^{-1} , which is higher than the calculated one (-13 kJ mol^{-1}).

Table 1: Rupture length, rupture force, desorption energy and binding energy for X₂₀ on gold

	Rupture length (nm)	Rupture force (pN)	Desorption energy (kJmol ⁻¹) (this study)	Binding energy (kJmol ⁻¹) (DFT)
A ₂₀	10 ± 2	78 ± 5 (180 ± 10)	23.6 ± 0.02 (54.6 ± 0.03)	-13
G ₂₀	10.3 ± 3	43 ± 5	13 ± 0.02	-17
C ₂₀	10 ± 3	44 ± 3	13.3 ± 0.01	-17
T ₂₀	11 ± 4	26 ± 3	7.8 ± 0.01	-5

T₂₄X₂ – Au interactions

To rule out the hypothesis that multiple nucleotides along the oligomer could interact with gold, we carried out a set of experiments with the same functionalization process except that the linker is a 24 bp homo-polymeric DNA strand of thymine with two units of adenine, cytosine, or guanine (i.e. T₂₄X₂, where X = A, C, and G). Following the same experimental protocol, we collected and analyzed force-distance curves for T₂₄X₂ (where X = A, C, or G) (Figure 2a). Histograms for these nucleotides are shown in Figure 2b, with force values of 47 ± 5, 54 ± 15, and 86 ± 2 pN for C, G, and A respectively. The rupture forces are consistent with the forces obtained for X₂₀ (Figure 1b). These results therefore indicate that only the last nucleotides at the extremity of the molecule interact with gold at the time of rupture. In addition, histograms of rupture lengths (Figure S2) for all DNA sequences show a unimodal distribution with mean peak values of 15 ± 4 nm, 13 ± 3 nm and 14 ± 3 nm for T₂₄C₂, T₂₄G₂ and T₂₄A₂, respectively further verifying our assessment of looking at the interaction between the X₂ extremity and gold. It is very unlikely that the last 2 nucleotides bind to the surface at the same time. The binding requires a perfect orientation of the species. If the last nucleotide is well-oriented to interact with the surface, the next one is not for geometry reasons (angle formed between four atoms, O5'-C5'-C4'-C3' (γ torsion) in the nucleic acid backbone of the single strand)¹⁵. We can also exclude the possibility that the broader distribution observed for A₂₀ (see previous section) is due to multiple interactions from several segments along the oligomer with gold. We can now attribute the second peak to another binding mode. It has been recently shown that the binding of DNA with adenine sequences is highly favorable on gold^{10,18} and it has been proposed that the interaction takes place via two main binding modes: physisorption and/or a weak chemical bond between the NH₂ groups and gold¹⁰. Furthermore, a SERS study on the coordination chemistry of DNA nucleosides with gold nanoparticles¹⁹ in water has shown that there exists a gold surface-adenine configuration which is relatively tight and corresponds to a very particular surface-adenine complex. Those results have shown that adenine is the only one that strongly interacts with the

gold surface through a complex coordination structure where the nitrogen atom of the imidazole ring binds to gold with the participation of the external amino group in the surface binding process. Our broad force distribution with two main peaks for the adenine interaction with gold is consistent with the fact that adenine is able to bind through both physisorption and chemisorptions^{10,17,18}. It shows that AFM SMFS is able to detect those two binding modes. To investigate into more details the involved interactions, we compared the rupture force of adenine-Au to the force of amine-Au in water (we used a pure aqueous solution without any buffer to compare our results with the SERS results described in ref. 18). The experimental protocol and tip functionalization process are unaltered, except that the linker is a 22 base heterogeneous DNA sequence with an amine group ($-\text{NH}_2$) at its terminal end (See Experimental section for details). In this set of experiments, we find a most probable force value of 134 ± 11 pN in force histograms for amine, in an excellent agreement with DFT calculations for ammonia and Au interactions²⁰. In Figure S3, we compare force histograms for adenine and $-\text{NH}_2$ terminal groups. These force histograms, which maximized at 237 pN and 134 pN for A and NH_2 , respectively, indicate that not only the NH_2 groups are responsible for the interaction with gold. They show that adenine indeed possesses much more stronger and asymmetrical interaction with Au than amine and other nucleobases (T, C and G).

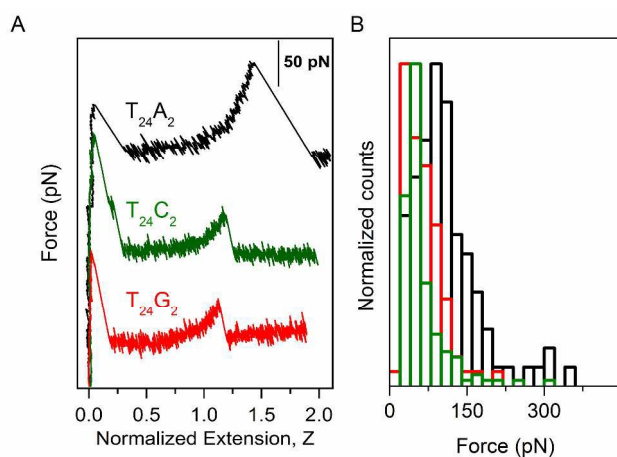


Figure 2: (A) Normalized force-extension curves of three $T_{24}X_2$ DNA strands showing the rupture of the bond formed between the nucleobases and Au in 150mM NH_4OAc . All curves are normalized to $Z=1$ at $F=20$ pN. (B) Histograms of rupture forces for $T_{24}A_2$ (black), $T_{24}C_2$ (green), and $T_{24}G_2$ (red).

Effect of ionic strength and surface dwell time

To investigate the effect of ionic strength on rupture forces, we evaluated force histograms at various NH_4OAc concentrations. We collected and analyzed large datasets of force-extension curves to determine the nucleotides-surface rupture forces. Histograms of rupture forces for three nucleotides (T_{24}A_2 , T_{24}C_2 and T_{24}G_2) at three salinity conditions are shown in Figure 3. We observe that the rupture forces increase when we decrease the ionic strength of the medium for all three cases. In Figure 4, we summarize the results for two surface dwell times and various NH_4OAc concentrations for all three nucleotides. From the evolution of the rupture force (Figure 4, left panels) it is evident that DNA bases detach from the gold surface at higher forces in low and medium salinity conditions, and that extending surface dwell time from 0.01s (Figure 4, close symbols) to 1s (Figure 4, open symbols), gives rise to a substantial increase in the bond rupture forces for the whole range of NH_4OAc concentrations, especially for T_{24}G_2 and T_{24}C_2 .

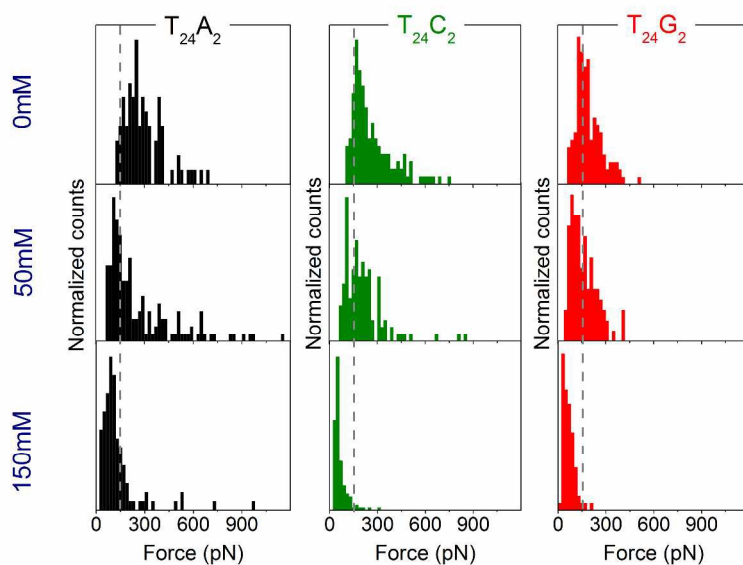


Figure 3: Histograms of rupture forces between nucleotides (T_{24}A_2 ; black, T_{24}C_2 ; green, and T_{24}G_2 ; red) and Au. Measurements were performed for three concentrations of NH_4OAc (0, 50, and 100 mM) and 0.01s of surface dwell time for all three nucleotides. The pH of all solutions was kept constant (i.e., pH 7)

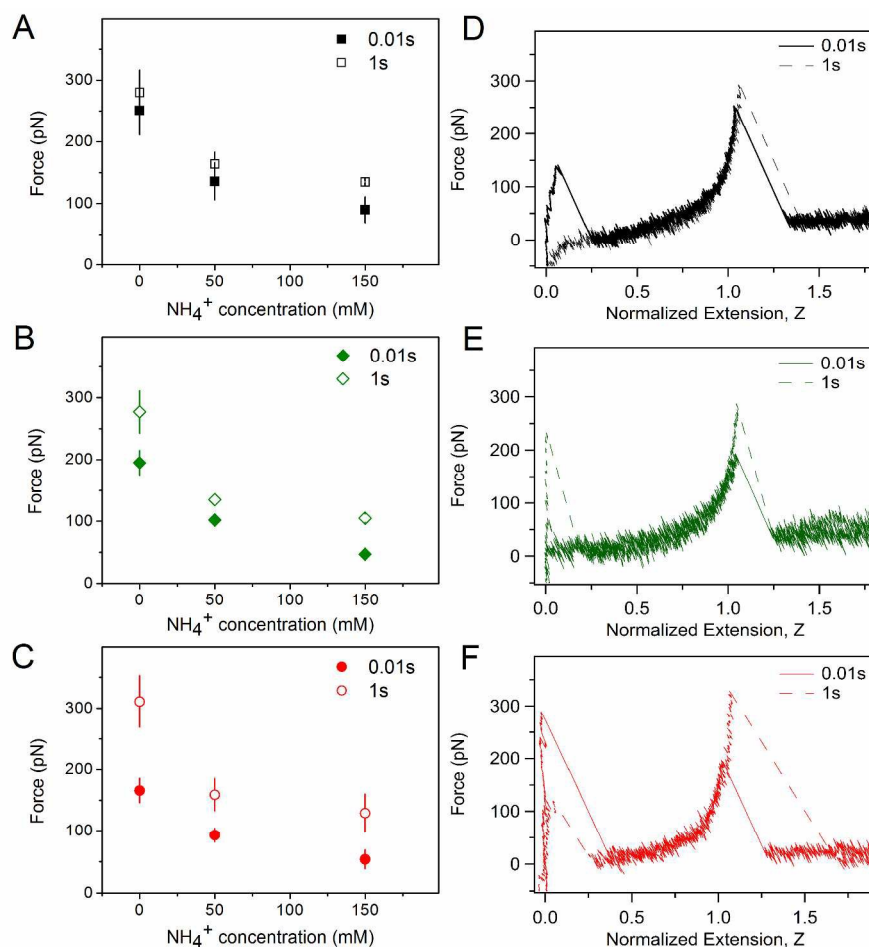


Figure 4: Force versus NH_4OAc concentration plots (A) T_{24}A_2 , (B) T_{24}C_2 , and (C) T_{24}G_2 for surface dwell time of 0.01s (closed symbols) and 1s (open symbols) with their corresponding normalized force-extension curves obtained in water (0mM, NH_4OAc) (D-F). The pH of all solutions was kept constant (i.e., pH 7).

In force histograms for surface dwell time of 1s, which are shown in Figure 5, we also found broader distributions in addition to the increase in rupture forces for all nucleotides. Although this increase could be due to the interactions of more than one molecule, the normalization of the force curves rules out this possibility (Figure S5), in line with the fact that the normalization of force curves can provide good evidence for single molecules detection²¹. In Figure 4 (right panel), we show normalized force-extension curves for T_{24}A_2 (in black), T_{24}C_2 (in green), and T_{24}G_2 (in red) that were registered in 0mM NH_4OAc for surface dwell times of 0.01s (solid lines), and 1s (dashed lines). These curves, which are normalized to $Z = 1$ nm at $F=150$ pN, show an increase of 95, 45, and 6 % in unbinding forces for guanine and cytosine, and adenine respectively.

These measurements, taken together with ionic strength data, allow us to conclude that low/medium salinity conditions are optimal for the strong adsorption of nucleotides on Au. It is

known that free ions distribute around charged objects (Au and DNA here) and form screening layers, which are extremely sensitive to the ionic strength. When low or medium salinity conditions deplete these layers and permit DNA bases to bind at preferred sites, strong base-Au interactions can take place and result in an increase of bond rupture forces. The higher rupture forces at extended surface dwell time for each concentration leave room for conception. The very small increase of the unbinding force for adenine is not surprising because adenine was shown to form a strong bond with gold even under physiological conditions (see previous sections). The high increase in force for guanine (95%) and cytosine (45%) could be the signature of chemisorption of these bases on Au. The formation of chemical bonds requires a perfect orientation of the partners, which could be achieved if we give enough time to them to find each other¹³. We can argue that this probability increases when the contact time increases.

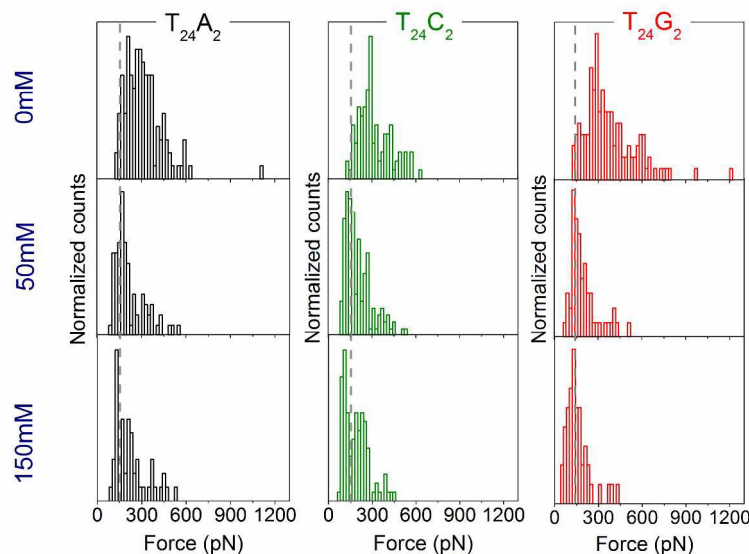


Figure 5: Histograms of rupture forces between nucleotides ($T_{24}A_2$; black, $T_{24}C_2$; green, and $T_{24}G_2$; red) and Au. Measurements were performed for three concentrations of NH_4OAc (0, 50, and 150 mM) and 1s of surface dwell time for all three nucleotides. The pH of all solutions was kept constant (i.e., pH 7).

CONCLUSIONS

Although DNA functionalized gold surfaces have attracted huge attention of researchers in many disciplines of nanotechnology and biotechnology, little is known about the forces that nucleotides-Au bonds can hold. Using AFM-based SMFS experiments, we quantified the nucleotides-Au bond strength in liquid and/or under physiological conditions. Force data show that, at physiological ionic strength, adenine-Au interactions are stronger, asymmetrical and

independent of surface dwell time, as compared to cytosine-Au and guanine-Au interactions. We suggest that in these conditions only adenine is able to chemisorb on gold. A decrease of the ionic strength of the medium significantly increases the bond strength for all nucleotides. We show that moderate ionic strength along with longer surface dwell period suggest weak chemisorption also for cytosine and guanine.

An exclusive feature of such measurements is the mechanical activation of ‘weak’ chemisorption, which can be probed at the single-molecule level. The ability to control and modulate the interaction of DNA-based molecules with inorganic surfaces is of crucial importance for future molecular devices and a multitude of biotechnological applications.

EXPERIMENTAL SECTION

Materials: All homo-polymeric DNA (X, where X= T, C, G, and A, SH-(CH₂)₆-5'-X₂₀-3') were purchased as HPLC purified grade from Biomers GmbH (Ulm, Germany) and DNA with the sequence T₂₄X₂ (SH-(CH₂)₆-5'-TTTTTTTTTTTTTTTTTTTTTTTTTTTXX-3', where X = A, C, and G) were all purchased as HPLC purification scale from Eurogentec S.A. (Belgium). The dried DNA samples were dissolved in MilliQ water (resistance > 18MΩcm, Millipore) to obtain a 100μM concentrated solution and were stored at -20°C. DNA (SHF₉-NH₂) used in the control experiment was kindly provided by Dr. Ljiljana Fruk, (KIT, Germany) and was used without further changes. The DNA sequence was (SH-(CH₂)₆-5'CTTCACGATTGCCACTTCCAC3'-NH₂). Potassium phosphate (KH₂PO₄) was purchased from Acros Organics and ammonium acetate (NH₄OAc) from Fluka. 6-mercapto-1-hexanol (MCH) was purchased from Sigma-Aldrich. Potassium phosphate (1M, pH = 4.7) and ammonium acetate (0-150mM, pH = 7) aqueous solutions were prepared in mQ water.

Surface preparation: Gold-coated Si wafers were purchased from Sigma-Aldrich. Prior to use, gold surfaces were cleaned by exposing to a UV light source (UV-Cleaner, Jelight company, Inc. USA) for 30 mins, rinsed abundantly with ethanol (Fisher Scientific), and blown dry in N₂. The cleaned surfaces were then immediately immersed in NH₄OAc buffer (0-150mM) to avoid long exposure to air.

Tip functionalization: Gold-coated silicon nitride cantilevers (BioLevers series), with nominal spring constants of 0.03-0.006 N/m were purchased from Olympus. After treating with UV light for 30 mins and rinsing with ethanol, AFM tips were incubated first in the solution of 1μM

thiolated ssDNA dissolved in 1M KH_2PO_4 (pH 4) for 10 minutes, and subsequently in the solution of 250 μM 6-mercapto-1-hexanol (MCH) dissolved in MilliQ water for 5 minutes. Our selection of 1M KH_2PO_4 buffer with pH = 4 for immobilization was chosen to ensure low coverage of thiolated ssDNA on gold as shown by others²². Thiol binds strongly to the gold, and allows the robust immobilization of ssDNA to the gold-coated tip for collecting more than ten thousand curves in a single experiment. The cantilevers were rinsed with copious amounts of MilliQ water, and immersed in 150mM NH_4OAc aqueous solution. All cantilevers were used immediately after the functionalization process.

AFM SMFS Measurements: All measurements were carried out with a PicoPlus 5500 (Agilent technologies, CA) using a liquid cell. The spring constants of all cantilevers were calibrated by using the built-in thermal software, and values were found in the range of nominal spring constants with less than 10% error. The AFM based SMFS theory and method of data analysis has been described in great extend elsewhere²³. Briefly, the experiment protocol for force-extension measurements consists of repeatedly forming and breaking DNA-Au bonds between the Au-coated AFM tips functionalized with thiolated ssDNA strands and the cleaned Au surface. The AFM tip was brought into contact with the Au surface and retracted at the speed of 100nm/s, in either NH_4OAc aqueous solution (pH 7) or MilliQ water containing traces of NaOH or HCl to adjust the pH to 7, so that force-extension curves of the ssDNA were recorded. The maximum force applied to the surface was fixed at 1 nN. All experiments were performed at room temperature. For each experiment dataset, we obtained the average rupture force value from a fit of the data (at least 200 curves recorded with 3 different but identically prepared cantilever and gold surfaces) with a probability density function, as well as a Gaussian mixture model (GMM, a weighted sum of M component Gaussian densities). See the details in ESI. The error in the reported force values was calculated using the following expression: $2\sigma/\sqrt{N}$, where σ is the width of force histograms and N is total number of rupture forces.

ELECTRONIC SUPPORTING INFORMATION

Details of the data analysis; Figures S1-S5; Histograms of rupture lengths; Histograms for Au-Adenine and Au-amine interactions; Force-extension curve for MCH-Au interactions; Normalized force-extension curves; Theoretical length of the DNA oligomers

AUTHOR INFORMATION

Corresponding Author

*(A-S. D) Email: asduwez@ulg.ac.be

Present Addresses

†Biosurfaces Unit, CIC biomaGUNE, 20009 San Sebastian, Spain

Notes

The authors declare no competing financial interest.

ACKNOWLEDGMENT

This research was funded by the Action de Recherche Concertée NANOFORCES (ARC 09/14 01).

REFERENCES

1. A. P. de Silva, S. S. K. de Silva, N. C. W. Goonesekera, H. Q. N. Gunaratne, P. L. M. Lynch, K. R. Nesbitt, S. T. Patuwathavithana and N. L. D. S. Ramyalal, *J. Am. Chem. Soc.*, 2007, **129**, 3050-3051.
2. M. V. Vincenzo Balzani, Alberto Credi *Molecular Devices and Machines: A Journey into the Nanoworld*, Wiley-VCH, 2006.
3. I. Willner, B. Shlyahovsky, M. Zayats and B. Willner, *Chem. Soc. Rev.*, 2008, **37**, 1153-1165.
4. S. K. Arya, P. R. Solanki, M. Datta and B. D. Malhotra, *Biosens. Bioelectron.*, 2009, **24**, 2810-2817.
5. A. B. Steel, R. L. Levicky, T. M. Herne and M. J. Tarlov, *Biophys. J.*, **79**, 975-981.
6. F. Bano, L. Fruk, B. Sanavio, M. Glettenberg, L. Casalis, C. M. Niemeyer and G. Scoles, *Nano Lett.*, 2009, **9**, 2614-2618.
7. E. Mirmomtaz, M. Castronovo, C. Grunwald, F. Bano, D. Scaini, A. A. Ensafi, G. Scoles and L. Casalis, *Nano Lett.*, 2008, **8**, 4134-4139.
8. L. M. Demers, M. Östblom, H. Zhang, N.-H. Jang, B. Liedberg and C. A. Mirkin, *J. Am. Chem. Soc.*, 2002, **124**, 11248-11249.
9. Li and L. J. Rothberg, *J. Am. Chem. Soc.*, 2004, **126**, 10958-10961.
10. M. Erdmann, R. David, A. R. Fornof and H. E. Gaub, *Nat. Chem.*, 2010, **2**, 745-749.
11. U. Rant, K. Arinaga, S. Fujita, N. Yokoyama, G. Abstreiter and M. Tornow, *Org. Biomol. Chem.*, 2006, **4**, 3448-3455.
12. F. W. Bartels, B. Baumgarth, D. Anselmetti, R. Ros and A. Becker, *J. Struct. Biol.*, 2003, **143**, 145-152.
13. A. S. Duwez, S. Cuenot, C. Jerome, S. Gabriel, R. Jerome, S. Rapino and F. Zerbetto, *Nat. Nanotechnol.*, 2006, **1**, 122-125.
14. R. Eckel, S. D. Wilking, A. Becker, N. Sewald, R. Ros and D. Anselmetti, *Angew. Chem., Int. Ed.*, 2005, **44**, 3921-3924.
15. Z. N. Scholl, M. Rabbi, D. Lee, L. Manson, S. G. H and P. E. Marszalek, *Phys. Rev. Lett.*, 2013, **111**, 188302-188305.
16. W. Lu, L. Wang, J. Li, Y. Zhao, Z. Zhou, J. Shi, X. Zuo and D. Pan, *Sci Rep*, 2015, **5**, 10158-10167.
17. S. Piana and A. Bilic, *J. Phys. Chem. B*, 2006, **110**, 23467-23471.
18. M. Erdmann, R. David, A. Fornof and H. E. Gaub, *Nat. Nanotechnol.*, 2010, **5**, 154-159.
19. N. H. Jang, *Bull. Korean Chem. Soc.*, 2002, **23**, 1790-1800.
20. A. Bilić, J. R. Reimers, N. S. Hush and J. Hafner, *J. Chem. Phys.*, 2002, **116**, 8981-8987.
21. A. Janshoff, M. Neitzert, Y. Oberdorfer and H. Fuchs, *Angew. Chem., Int. Ed.*, 2000, **39**, 3212-3237.

22. D. Y. Petrovykh, H. Kimura-Suda, L. J. Whitman and M. J. Tarlov, *J. Am. Chem. Soc.*, 2003, **125**, 5219-5226.
 23. T. Puntheeranurak, I. Neundlinger, R. K. Kinne and P. Hinterdorfer, *Nat. Protoc.*, 2011, **6**, 1443-1452.
-